Wireless Netw
DOI 10.1007/s11276-014-0698-x

Path diversified multi-QoS optimization in multi-channel wireless mesh networks

Xiaoyuan Guo · Feng Wang · Jiangchuan Liu · Yong Cui

Abstract Wireless mesh networks (WMNs) have become a promising solution for quick and low-cost spreading of Internet accesses and other network services. Given the mesh topology, multiple paths are often available between node pairs, which thus naturally endorse path-diversified transmission. Unfortunately, like in wired networks, discovering completely disjoint paths in a WMN remains an intractable problem. It indeed becomes more challenging given the interferences across wireless channels in a WMN, not to mention that applications may demand heterogeneous QoS optimizations across different paths. The availability of multiple channels in advanced WMNs however sheds new lights into this problem. In this paper, we show that, as long as the best channels with different QoS metrics are not overlapped between neighboring node pairs, complete disjoint paths with heterogeneous QoS targets are available in a multi-channel WMN. We present efficient solutions to discover such paths, particularly for bandwidth- and delay-optimization. We also develop novel algorithms for accurately estimating path bandwidth and delay in the multi-channel environment. These lead to the design of a practical protocol that extends the classical Ad hoc On-demand Multi-path Distance Vector (AOMDV). Through extensive simulations, we show that our protocol yields significant improvement over state-of-the-art multi-path protocols in terms of both end-to-end throughput and delay.

Keywords Multi-QoS · Multi-channel · Multi-path routing · Wireless mesh network

1 Introduction

The recent advances in multi-hop broadband wireless networking have made wireless mesh networks (WMNs) [1] a promising solution for quick and low-cost spreading of Internet accesses and other network services in personal, local, and old metropolitan areas. Given the mesh topology of a WMN, multiple paths are often available between node pairs, thus naturally endorsing path-diversified transmission [2–4], which can exploit multiple routes simultaneously for a connection, achieving higher aggregated bandwidth and potentially decreasing delay and packet loss. Unfortunately, like in wired networks, discovering completely disjoint paths in a WMN remains an intractable problem [5–7].

Furthermore, conventional multi-path protocols have largely focused on path selection with homogeneous QoS, typically the path bandwidth. Yet for many applications, paths with different QoS optimizations would enable much better flexibility toward traffic split and thus better end-to-end performance. As an example, the retransmitted data of a TCP flow would prefer a delay-minimized path, while the original data, which is generally of larger volume, would

X. Guo · J. Liu
School of Computing Science, Simon Fraser University, Burnaby, BC, Canada
e-mail: xxg1@cs.sfu.ca

J. Liu
e-mail: jcliu@cs.sfu.ca

F. Wang (✉)
Department of Computer and Information Science, The University of Mississippi, University, MS, USA
e-mail: fwang@cs.olemiss.edu

Y. Cui
Department of Computer Science and Technology, Tsinghua University, Beijing, China
e-mail: cuiyong@tsinghua.edu.cn

Published online: 06 February 2014

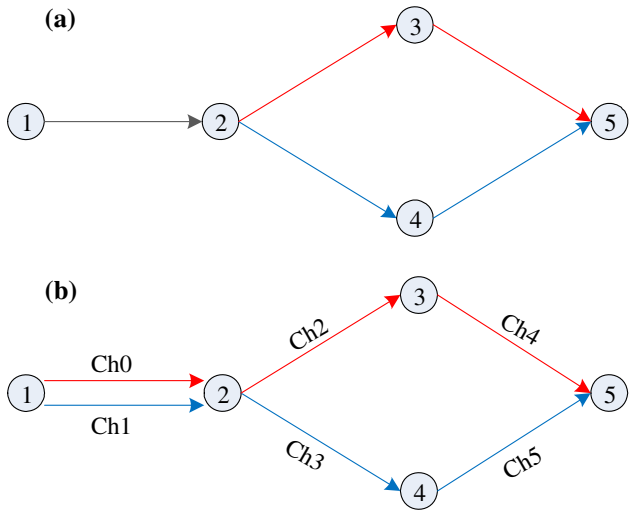

Fig. 1 Illustration for benefits of multi-channel to multi-path routing. (**a**) Single channel case. Two overlapping paths between sender 1 and receiver 5. Path 1: $1 \rightarrow 2 \rightarrow 3 \rightarrow 5$. Path 2: $1 \rightarrow 2 \rightarrow 4 \rightarrow 5$. (**b**) Multiple channel case. Two disjoint paths between sender 1 and receiver 5. Path 1: $1^0 \rightarrow 2^0 \rightarrow 3 \rightarrow 5$; Path 2: $1^1 \rightarrow 2^1 \rightarrow 4 \rightarrow 5$

prefer a bandwidth-maximized path. For video transmission over UDP, to ensure smooth realtime playback, the critical I-frames may prefer a delay-minimized path, while others can be delivered through a bandwidth-maximized path. It is known that multi-QoS optimization is a difficult problem [5, 8–11], and it indeed becomes more challenging given the interference across wireless channels in a WMN.

The availability of multiple channels in advanced WMNs however sheds new lights into these problems. Disjoint paths with heterogeneous QoS optimizations can be readily available in a multi-channel WMN. As illustrated in Fig. 1(a), in the single channel case, *link 2–3* and *link 2–4* will interfere with each other (so do *link 3–5* and *4–5*), and the overlapping *link 1–2* in *path 1* and *path 2* can be a bottleneck. On the other hand, if the links can operate on different channels (say, 6) simultaneously as in Fig. 1(b), then *link 2–3* and *link 2–4* will have no interference, and *path 1* and *path 2* will be disjoint with each other completely.

In this paper, we show that, as long as the best channels with different QoS metrics are not overlapped between WMN node pairs, there exist complete disjoint paths with different QoS metrics. We present efficient solutions to discover such paths, particularly for bandwidth- and delay-optimization. Note that the existence of multiple channels notably changes the interference pattern from that in single-channel WMNs, rendering the existing bandwidth and delay estimate tools [12–15] far from being accurate. Our joint optimization of bandwidth and delay (JOBD) protocol offers novel estimation tools that take both intra- and inter-flow interferences under channel diversity into account, achieving much more accurate bandwidth and delay estimations in the multi-channel WMN environment. We have discussed a series of practical issues toward implementing the JOBD protocol, and evaluated its performance through *ns*-2 simulations. The results demonstrate that, by distributing traffic over different QoS-optimized paths, our JOBD protocol yields significant improvement over state-of-the-art multi-path protocols in terms of both end-to-end throughput and delay.

The remainder of this paper is organized as follows. Section 2 reviews the background and related work. In Sect. 3, we present our system model and analyze the joint optimization problem of bandwidth and delay in multi-channel multi-path WMNs. Section 4 develops new algorithms to estimate bandwidth and delay under channel diversity. Section 5 discusses the practical implementation issues of the JOBD protocol. Its performance is evaluated in Sect. 6. Finally, Sect. 7 concludes the paper and points out future directions.

2 Background and related work

A number of recent deployments of WMNs have been witnessed, and diverse networked applications are now running over these networks [7, 16, 17]. Unfortunately, their end-to-end performance is often unsatisfactory due to the limited bandwidth, strong interference among the wireless nodes, and unavoidable collision caused by hidden and exposed terminals. To this end, there have been significant studies on finding routes with diverse QoS guarantees [5, 8, 18–21], where Wang and Crowcroft [5] first proved that multi-constraint-path selection in single-path routing is a NP-complete problem and gave three heuristic path computation algorithms.

Later, path diversity was proposed to exploit multiple routes simultaneously for a connection, achieving higher aggregated bandwidth and potentially decreasing delay and packet loss. Given the mesh topology of a WMN, multiple paths are often available between node pairs, thus naturally endorsing path-diversified transmission. Wang et al. [22] argued that the paths should be disjoint, otherwise network performance enhancement would be bottlenecked. Fully disjoint paths (node-disjoint and link-disjoint paths) however are not always available in a network. Maximally disjoint QoS paths are therefore suggested as an approximation and various heuristic algorithms were proposed [23–25]. The interference among multiple paths, a key factor in wireless transmission, has not been addressed in these works.

Multi-channel has been suggested as an important technique to significantly reduce the wireless interference and improve network capacity in WMNs [1]. Much effort

has been devoted to utilizing multi-channel in multi-path routing in this context [2–4, 26, 27], but mainly focusing on homogeneous QoS. New routing metrics that capture the intra/inter-flow interference under channel diversity in WMNs have also been examined in [12–15]. Weighted cumulative expected transmission time (WCETT) [12] combines link weights with expected transmission time (ETT) to account for intra-flow interference, where ETT is derived based on link loss rate and bandwidth. Weighted end-to-end delay (WEED) [15] estimates the end-to-end delay with respect to intra-flow and inter-flow interference through a sub-path abstraction, where only intra-flow interference between two adjacent links are calculated. In stead, we consider a much more complicate but more real scenario that beside inter-flow interference, intra-flow interference exists among all links in one flow path, resulting in better performance. To the best of our knowledge, our paper is the first work that employs multi-channel to utilize bandwidth- and delay-optimized disjoint paths simultaneously in WMNs.

3 System overview and problem statement

We consider a WMN of K nodes (wireless routers), in which any two nodes can communicate directly or through multi-hop relays. Each node is configured with N full-duplex wireless interfaces ($N \geq 2$) [28–30]. There are also N orthogonal channels in the WMN and each interface is allotted with one channel.[1] We refer to each channel between two neighboring nodes as a *channel link*, or a *link* in short. Hence, there are N links between two neighboring nodes in our system, as illustrated in Fig. 2 where $N = 2$.

The goal of our multi-channel multi-path routing protocol is to find two disjoint paths with different QoS-optimized performance. We are particularly interested in bandwidth and delay, although our solution framework is general in accommodating other QoS parameters.

We transform the WMN into a weighted undirected graph $G(V, E)$ as shown in Fig. 3, where V is the set of nodes and E is the set of links. In particular, V consists of two kinds of nodes, namely, *master nodes* (or *M-nodes* in short) and *interface nodes* (or *I-nodes* in short), representing the nodes and their interfaces in the WMN, respectively. Let V_m denote the set of M-nodes, and V_i denote the set of I-nodes. Obviously, every M-node has N I-nodes and only the nodes in set V_m can be selected as source s and destination t. The edges are also categorized

[1] These interfaces are identical with the same transmission and carrier sensing range, and can be switched from one channel to another within marginal delay. In practice the number of channels can be more than that of interfaces, and there have been a number of dynamic channel assignment algorithms available [31–34].

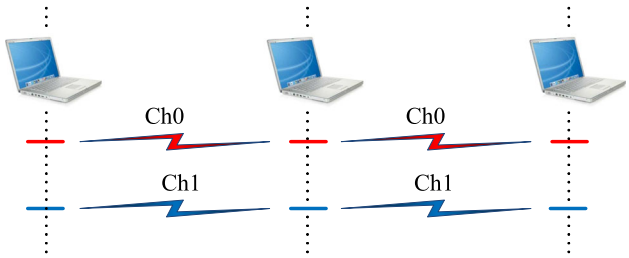

Fig. 2 A multi-channel WMN with 3 nodes. Each node is configured with two channels, and thus there are two links between neighboring nodes

into two sets, E_m and E_i. The edges in E_m are between M-nodes and their I-nodes. The edges in E_i are from every I-node of a M-node to the I-node of other M-nodes if two interfaces of different nodes operate on the same channel and within each other's transmission range in the WMN. Every edge e in E has two costs, namely, its available bandwidth and delay. Let $Bw(e)$ be the available bandwidth of e, $Delay(e)$ be the delay of e, and $C(e)$ be the channel capacity of e. We have $Bw(e) = \infty$ and $Delay(e) = 0$ if $e \in E_m$, as interfaces are switchable with marginal latency in one node in the WMN so that bandwidth approaches infinity. For $e \in E_i, 0 \leq Bw(e) \leq C(e)$ and $Delay(e) \geq 0$.

Let $P_{s,t}$ denote a loop-free path from source s to destination t as a set of edge sequence, i.e., $P_{s,t} = \{e_0, e_1, \ldots, e_l\}$, where for two neighboring edges $e_i = (x_i, y_i)$ and $e_{i+1} = (x_{i+1}, y_{i+1})\ (i = 0, \ldots, l-1)$, we have $y_i = x_{i+1}$. Also, we have $x_0 = s$ for $e_0 = (x_0, y_0)$ and $y_l = t$ for $e_l = (x_l, y_l)$. The bandwidth- and delay-optimized disjoint path selection problem in multi-channel WMNs can then be formulated as follows:

Given network $G(V,E)$, a source node s and a destination node t $(s, t \in V_m)$, find two paths $P_{s,t}^{bw}$ and $P_{s,t}^{delay}$ such that

$$P_{s,t}^{bw} \cap P_{s,t}^{delay} \cap E_i = \emptyset,$$

with objective function

$$\max\left(\min_{e \in P_{s,t}^{bw}} Bw(e)\right)$$

and

$$\min\left(\sum_{e \in P_{s,t}^{delay}} Delay(e)\right).$$

Theorem 1 *There exist complete disjoint paths with bandwidth- and delay-optimized performance, if the bandwidth- and delay- optimized channel links are different between neighboring nodes.*

Proof If the the bandwidth- and delay-optimized paths do not share any neighboring node pairs, the two paths are

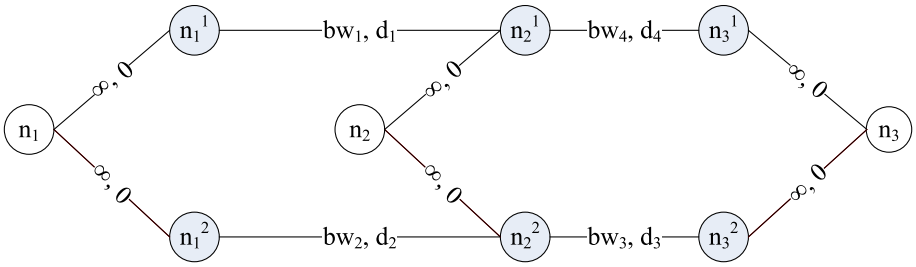

Fig. 3 A multi-channel WMN with 3 nodes, n_1, n_2 and n_3. Each node is configured with two interfaces. Each interface is considered as an I-node and connected to its M-node by an edge with infinite bandwidth and zero delay. Bandwidth and delay on other edges are also shown as bw_i and d_i, respectively. We assume $bw_1 > bw_2$, $d_1 > d_2$, $bw_3 > bw_4$, $d_3 > d_4$. If n_1 is the source node and n_3 is the destination, the maximum-bandwidth path will be $n_1 \rightarrow n_1^1 \rightarrow n_2^1 \rightarrow n_2 \rightarrow n_2^2 \rightarrow n_3^2 \rightarrow n_3$ and the minimum-delay path will be $n_1 \rightarrow n_1^2 \rightarrow n_2^2 \rightarrow n_2 \rightarrow n_2^1 \rightarrow n_3^1 \rightarrow n_3$

Table 1 List of notations

$G(V, E)$	A graph with V as its vertex set and E as its edge set
V_m	Set of M-nodes
V_i	Set of I-nodes
E_m	Set of edges between M-nodes and their I-nodes
E_i	Set of edges between I-nodes
$Bw(e)$	Available bandwidth of edge e
$C(e)$	Channel capacity of edge e
$Delay(e)$	Delay of edge e
$P_{s,t}^{bw}$	Maximum-bandwidth path from node s to t
$P_{s,t}^{delay}$	Minimum-delay path from node s to t
CHB_i	Channel busy time ratio for link i
ACB_i	Accumulated channel busy time for link i
T_{total}	Total channel time slot
B_i	Channel capacity of link i
B_{ITF_i}	Available bandwidth of link i in inter- flow interference
ETX_i	Expected transmission count in link i
TB_i	Channel busy time of link i
$TB_{1,2,\ldots,k}$	Accumulated channel busy time over links $1, 2, \ldots$, and k
B_{IAF}	Available bandwidth of a path in intra- flow interferece
D_p	End-to-end delay over path p
H	Hop count of path p
D_i	One hop delay of link i
I	Packet length
AB_i	Available bandwidth of link i
W_j	Contention window at the *jth* bankoff stage
M_i	Number of packets queued in the buffer of link i

clearly disjoint. Otherwise, for each overlapped neighboring node pair, the two paths can respectively pick up the bandwidth- and delay-optimized channel link between the two neighboring nodes and thus the two QoS-optimized paths are disjoint with no overlapped channel links. Note that node disjunction is not a requirement here, given the multiple interfaces can operate simultaneously in a node.

Given the above theorem, the disjoint path selection problem can be simply transformed into the classical max-flow problem and the shortest-path problem, respectively, and then solved separately.

One concern here is that the bandwidth-optimized link might overlap with the delay-optimized link between neighboring nodes. We however find this is not necessarily the case. While a high bandwidth link has lower transmission delay, the total delay of a link depends on many other factors, in particular, the number of packets that have queued for transmitting over the channel. Existing works [35, 36] have suggested that the latter is often the dominating factor, which is also confirmed by our analysis (see Sect. 6.1). As such, the probability that the two channel links overlap can be quite low if there are a number of channels available in the network (for IEEE 802.11a standard, there are 12 orthogonal channels).

A more critical challenge however is the accurate estimation of bandwidth and delay in this multi-channel environment. It is known that co-channel interference is dominating when multiple channels are available, which unfortunately has not been well addressed by state-of-the-art estimation algorithms [15, 37]. In the next section, we will address this challenge and develop more accurate estimation tools under channel diversity, and we will further present a practical protocol design in Section 5. To facilitate our discussion, Table 1 summarizes the key notations used in this paper.

4 Bandwidth and delay estimation under channel diversity

We proceed with new algorithm designs for computing the two routing metrics in the multi-channel environment, i.e., available bandwidth and end-to-end delay of a path. It is known that, due to the limitation of available orthogonal channels, with the existence of *co-channel links*, i.e., the

links operating on the same channel, both inter-flow interference and intra-flow interference can occur [13]. The former refers to the contentions that occur among co-channel links in different paths, and the latter refers to the contentions when co-channel links locate in the same path. We will first compute the available bandwidth under inter-flow interference and intra-flow interference separately, and then integrate them together to calculate the available bandwidth over a whole path. The computation of end-to-end delay will then be investigated afterwards.

4.1 Available bandwidth under inter-flow interference

We compute available bandwidth of link i under inter-flow interference, B_{ITF_i}, as follows:

$$B_{ITF_i} = \frac{(1 - CHB_i)B_i}{ETX_i}, \tag{1}$$

where B_i is channel capacity of link i, $CHB_i = \frac{ACB_i}{T_{total}}$ is *channel busy time ratio*, ACB_i is *accumulated channel busy time* of links inter-flow interfered with link i, T_{total} is total channel time slot including both "busy" and "idle" periods, and ETX_i represents *expected transmission count* required to successfully deliver a packet along link i. Obviously, $1 - CHB_i$ indicates channel idle ratio for link i, and the numerator part of B_{ITF_i} can be interpreted as the available bandwidth for one transmission. As such, B_{ITF_i} gives the effective available bandwidth for one successful transmission with ETX_i transmission attempts.

Note that the accumulated channel busy time, ACB_i, can not simply be the sum of all the channel busy time of links that suffer from inter-flow interferences with link i, since these links may have no interference with each other. If two co-channel links, m and n, do not locate in each other's interference range (such as links m_5 and n_1 in Fig. 4), their accumulated channel busy time will be in the range of $[\max(TB_m, TB_n), TB_m + TB_n]$ as TB_m and TB_n are independent with each other, where TB_m and TB_n are their channel busy times, respectively. And we can view their accumulated channel busy time TB_{mn} as a uniformly distributed random variable in $[\max(TB_m, TB_n), TB_m + TB_n]$ approximately. It follows that $E[TB_{mn}] = (TB_m + TB_n + \max(TB_m, TB_n))/2$. Otherwise, if m and n interfere with each other (such as links m_2 and n_1 in Fig. 4), TB_{mn} can simply be the sum of their channel busy time, since TB_m and TB_n could not occur simultaneously. In general, if co-channel links $l_1, l_2, \ldots$, and l_k have no interference with each other (note that these links all have co-channel interference with a common link), the accumulated channel busy time $TB_{1,2,\ldots,k}$ complies with uniform distribution in $[\max(TB_1, TB_2, \ldots, TB_k), \sum_{l=1}^{k} TB_l]$ approximately, and

$$E[TB_{1,\ldots,k}] = \frac{\sum_{l=1}^{k} TB_l + \max(TB_1, TB_2, \ldots, TB_k)}{2} \tag{2}$$

Therefore, we first divide the set of all links inter-flow interfering with link i into a minimum number of subsets, where the links do not interfere with each other in every subset but have interference with links in other subsets. For any subset S_j, the accumulated channel busy time ACB_{ij} is calculated according to Eq. (2), and the subset is viewed as a newly mixed virtual link with ACB_{ij} as its channel busy time. The overall accumulated channel busy time is the sum of the accumulated channel busy time of each subset, for there are interferences across links in different subsets. This calculation is summarized in Algorithm I.

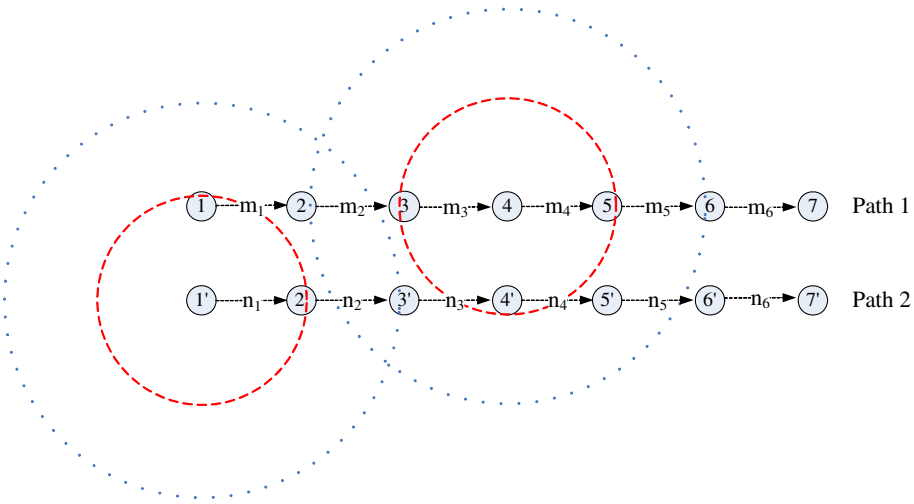

Fig. 4 Example of inter-flow interference between two paths. Assume links m_2, m_5 and n_1 are assigned with the same channel. The *small circle* covers available transmission range of a node, and the *large circle* denotes interference range of a node. So links m_2 and n_1 will suffer from co-channel inter-flow interference, while m_5 and n_1 have no such interference

4.2 Available bandwidth under intra-flow interference

When there are two co-channel links that interfere with each other in the same path, the two links can not transmit data simultaneously. The total transmission time of two links is the sum of the transmission time in each link. Assuming the size of the transmitted data is S_{data}, we thus have

$$\frac{S_{data}}{B_{i,j}} = \frac{S_{data}}{B_i} + \frac{S_{data}}{B_j}$$

where link i and link j are two interfered co-channel links in the same path, B_i and B_j are bandwidth of each link, and $B_{i,j}$ is the total available bandwidth over the two links. By dividing both sides of the equation with S_{data}, we then have

$$\frac{1}{B_{i,j}} = \frac{1}{B_i} + \frac{1}{B_j} \tag{3}$$

Similarly, for the scenario that co-channel links $l_1, l_2, \ldots$, and l_k interfere with each other in the same path, we have

$$\frac{1}{B_{l_1,l_2,\ldots,l_k}} = \frac{1}{B_{l_1}} + \frac{1}{B_{l_2}} + \ldots + \frac{1}{B_{l_k}} \tag{4}$$

where $B_{l_1,l_2,\ldots,l_k}$ is the total available bandwidth over links $l_1, l_2, \ldots$, and l_k.

As such, we can first find all the links that interfered with a particular link in one path. The available bandwidth of that link is then calculated by Eq. (4) and we then take the minimum available bandwidth among all links as the available bandwidth for that multi-channel path under intra-flow interference, as illustrated in Algorithm II. This is a centralized algorithm to be executed by the last node in one path. We further extend it to a distributed implementation, which considers two adjacent co-channel links at a time and thus can be executed hop-by-hop (see Algorithm III). Note that, in both algorithms, the co-channel links are sorted by their distances from the source, following the flow direction.

The path available bandwidth from Algorithm III can be slightly smaller than that from Algorithm II, since one link might be involved in Eq. (3) several times while it actually should just be involved in Eq. (4) one time. Nevertheless, state-of-the-art channel assignment algorithms are quite effective in minimizing the number of co-channel interfered links [38], and hence the difference of the two algorithms is marginal. Our experience is that the number of co-channel links interfering with each other is hardly beyond two.

Algorithm I Channel Busy Time for Individual Link under Inter-Flow Interference

Let TB_j be the channel busy time of link j
Let S be the set of links that inter-flow interfere with link i
Let ACB_i be the accumulated channel busy time for link i
Divide S into a minimum number (denoted as m) of subsets, where links have no interference with each other in every subset but interfere with links in other subsets, denoted as $S_1, S_2, ..., S_m$.
for $j = 1$ to m
  Suppose there are k links in subset S_j
  $ACB_{ij} = \frac{\sum_{l=1}^{k} TB_l + \max(TB_1, TB_2, ..., TB_k)}{2}$
end for
$ACB_i = \sum_{j=1}^{m} ACB_{ij}$

Algorithm II Centralized Algorithm for Available Bandwidth under Intra-Flow Interference

Let m be the number of different channels in one path
Let S_i be the set of links using channel i
Let $S^{'}$ be an empty set
Let $B_{IAF_{ij}}$ be the available bandwidth for link j using channel i
Let B_{IAF_i} be the available bandwidth for the links using channel i
Let B_{IAF} be the available bandwidth over a multi-channel path under intra-flow interference
for *i=1* **to** m
  $S_i^{'} = S_i$
  for link j in S_i with the smallest hopcount from the sender
    Suppose there are p links in set $S_j^{'}$ interfere with j, denoted as $l_1, l_2, ...l_p$
    $\frac{1}{B_{IAF_{ij}}} = \frac{1}{B_{l_1}} + \frac{1}{B_{l_2}} + ... + \frac{1}{B_{l_p}} + \frac{1}{B_j}$
    Remove link j from S_i
  $B_{IAF_i} = min(B_{IAF_{11}}, B_{IAF_{ij}})$
  end for
  $B_{IAF} = min(B_{IAF_1}, B_{IAF_i})$
end for

4.3 Available bandwidth over a multi-channel path

Taking both inter-flow and intra-flow interference into account, the available bandwidth over a multi-channel path can be evaluated by integrating Algorithm I and Algorithm III. Specifically, We replace the channel capacity PB_{ij} in Algorithm III with the available bandwidth of the *jth* link under inter-flow interference, which is obtained by

Algorithm I and Eq. (1). The B_{IAF} given by Algorithm III then becomes the available bandwidth over the multi-channel path.

Algorithm III Distributed Algorithm for Available Bandwidth under Intra-Flow Interference

Let m be the number of different channels in one path
Let n_i be the number of links using channel i
Let PB_{ij} be the channel capacity for the jth link under channel i
Let B_{IAF_i} be the available bandwidth for the links using channel i
Let B_{IAF} be the available bandwidth over a multi-channel path under intra-flow interference
for $i=1$ **to** m
  for $j=1$ **to** n_i
    if two adjacent co-channel links within interference range
      $\frac{1}{B_{IAF_i}} = \frac{1}{B_{IAF_i}} + \frac{1}{PB_{ij}}$
    else
      $B_{IAF_i} = min(B_{IAF_i}, PB_{ij})$
    end if
  end for
  $B_{IAF} = min(B_{IAF_1}, B_{IAF_i})$
end for

4.4 End-to-end delay over a multi-channel path (MC-EED)

The end-to-end delay is not only determined by path bandwidth, but also depends on other factors such as MAC access delay, and queuing delay [36]. To capture these factors, we compute the end-to-end delay of a path p as follows,

$$D_p = \sum_{i=1}^{H} D_i,$$

with

$$D_i = \left(ETX_i \frac{I}{AB_i} + \sum_{j=1}^{ETX_i} E[W_j] \right) \cdot M_i \quad (5)$$

The parameters here are summarized as follows, and the practical estimation of the key parameters will be detailed in the next section:

- D_p: end-to-end delay over path p;
- H: hop count of path p;
- D_i: one hop delay in link i;
- I: packet length;
- ETX_i: expected transmission count along link i;
- AB_i: available bandwidth of channel link i;
- W_j: contention window at the jth backoff stage;
- M_i: number of packets queued in the buffer of link i.

It is worth noting that in Eq. (5), AB_i is the available bandwidth of channel link i, which is mainly influenced by co-channel interferences and different from that in single-channel networks. The computation of AB_i adopts the algorithms proposed in the previous subsection. Specifically, we first find all the links inter-flow interfered with link i, and obtain the available bandwidth of link i under inter-flow interference according to Eq. (1). We then discover co-channel links interfered with link i in path p, and get AB_i through Eq. (4). According to the 802.11 standard [39, 40], $E[W_j] = (2^{j-1}W_{min} - 1)/2$, where W_{min} is the minimum contention window.

Intuitively, in Eq. (5), $ETX_i\frac{I}{AB_i}$ denotes the transmission delay under channel diversity, $\sum_{j=1}^{ETX_i} E[W_j]$ represents the MAC access delay, and M_i captures the queuing delay. Note that AB_i is the available bandwidth of channel link i rather than the available bandwidth of the whole path p. Comparing Algorithm III with Eq. (5), we can easily find that the delay is not simply inversely proportional to the available bandwidth of one path.

5 JOBD routing protocol design

In this section, we present a practical protocol design, JOBD, that incorporates the above results for discovering and utilizing the maximum-bandwidth path and the minimum-delay path simultaneously.

5.1 Basic AOMDV

Our JOBD protocol inherits the route discovery mechanism from the Ad hoc On-demand Multi-path Distance Vector (AOMDV) protocol [41], a well-known multi-path extension to the classical AODV. AOMDV computes multiple loop-free and link-disjoint paths with customized flooding, and takes hopcount as its routing metric. In AOMDV, a node records the maximum hopcount of the multiple paths for each destination, referred to as the *advertised hopcount* for that destination. The protocol only picks up alternative routes with hopcount less than the *advertised hopcount*. The *first hop* field in an AOMDV Route REQuest packet (RREQ) or Route REPly packet (RREP), which indicates the first hop taken by the packet, is used to ensure the disjunction of the multiple paths.

5.2 Route discovery in JOBD

In our JOBD protocol, when a node has data to transmit, it first broadcasts a *route request* message (RREQ) through

all its interfaces. To discover QoS-optimized routes, we extend the header of each RREQ packet to ⟨*bw*, *delay*, *chan-bw*, *last-chan-ID*, AOMDV RREQ header⟩, as shown in Fig. 5. Here, *bw* and *delay* are the available bandwidth and end-to-end delay of the path passed by this RREQ, *chan-bw* records the available bandwidth for each channel, and *last-chan-ID* indicates last channel it passes. When one interface of an intermediate node receives an RREQ message at the first time, the node first gets the value of its channel (channel number is *last-chan-ID*) available bandwidth and one hop delay. It then updates *chan-bw*, the bandwidth of the channel. The *bw* is determined by the minimum bandwidth among all channels recorded in *chan-bw*. The *delay* field is updated similar as that of *hopcount* in the AOMDV header.

The node then rebroadcasts the message through all of its interfaces. Redundant RREQ messages can be used to build multiple reverse paths. Once the destination receives an RREQ packet, it updates the *bw* and *delay* fields as intermediate nodes, establishes the reverse path, and sends back RREP along the newly built reverse path. Subsequently, the destination or the nodes that have routes to the destination send back RREP packets with newly modified

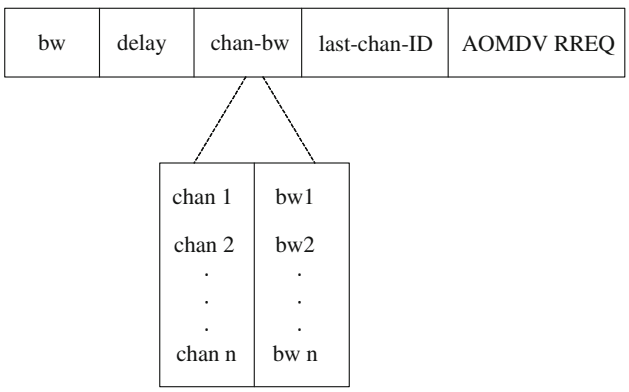

Fig. 5 JOBD RREQ packet header

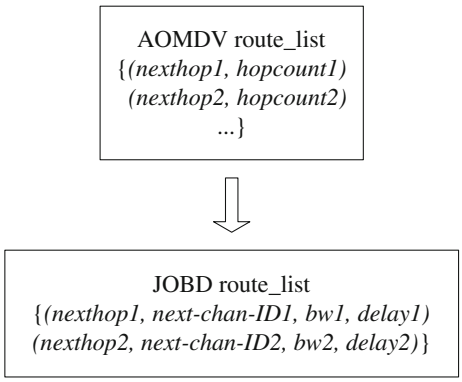

Fig. 6 The route list of AOMDV and JOBD

packet header, ⟨*bw*, *delay*, *last-chan-ID*, AOMDV RREP header⟩, to assist establishing forwarding paths. The three new fields in RREP have the same meanings as those in RREQ packet header.

The routing table entries are also redesigned in JOBD. Specifically, we add *next-chan-ID*, *bw* and *delay* fields in route_list, as illustrated in Fig. 6. These three new fields indicate the channel number of next hop, the available bandwidth, and the end-to-end delay of one route, respectively. Similar to AOMDV, a route is updated when a node receives a RREQ or RREP packet with a new *sequence number* or there's a better path, e.g., with larger achievable bandwidth or smaller end-to-end delay.

5.3 Parameter estimation

A key step toward implementing JOBD is the estimation of the two path selection metrics, namely, available bandwidth and end-to-end delay. Given the algorithms in Section 4, this can be accomplished by measuring *ETX*, channel busy time, and the number of packets queued in the buffer.

To calculate *ETX*, we need to obtain the forward and reverse delivery ratio (d_f and d_r). The value of d_f and d_r can be evaluated through link probing [42]. Each node periodically broadcasts probing packets, say, at a rate of one packet per second. Every node records the number of probing packets it receives during last ten seconds and inserts this information in the header of its own probe packets. Therefore, the nodes can compute d_r directly from the number of packets they receive during a recent period, say, ten seconds, and also obtain d_f by using the information in the probe packets sent to themselves from one of their neighbors.

For the measurement of channel busy time, we take the time that packets are sent successfully from one node along one channel as the busy time of that channel in a certain time period.

The number of packets queued in the buffer can also be estimated through probing packets [15]. Specifically, each node periodically broadcasts probing packets to its downstream neighbors at a predetermined rate, carrying over the number of packets queued in the buffer in its probe packet header. When downstream nodes receive the probing packets, they will update the count of packets queued in their upstreaming nodes in their neighbor lists.

6 Performance evaluation

In this section, we evaluate the performance of our solution through *ns*-2 simulations. We adopt a similar configuration as in [15, 43, 44]. Specifically, we conduct experiments on

both random and grid topologies. The random topology consists of 40 nodes uniformly distributed in a 1,000 m × 1,000 m area, where 8 flows are run over the network. The grid topology places 100 nodes with a distance of 200 m between two adjacent nodes and 10 flows are operated across the network. In both topologies, the sources and destinations of all flows are randomly picked. Each node is configured with 250 m as its transmission range and 500 m as its interference distance. The MAC protocol adopts 802.11a with 5 Mbps as its channel rate. We use the channel assignment scheme proposed by Kyasanur et al. [34] and configure 12 channels with 4 interfaces for each node. We implemented separate buffer queues for each interface. To mitigate randomness, for each topology, we run 100 simulations with different source and destination selections, and for random topology, a new network topology is also generated for each simulation. The results shown in the figures are thus the average of 100 simulations.

For comparison, we also implement another two state-of-the-art multi-path routing protocols. One is AOMDV [41], which is a well-adopted protocol for multi-path routing in the single channel environment. And we further extend it to support multi-channel in our evaluation. The other protocol is a multi-channel multi-path routing protocol proposed in [26]. To further improve its performance, we use a modified version that also uses WEED [15] as the routing metric and we denote the resulting protocol as MWEED.

In the following subsections, we first examine the probability that bandwidth- and delay-optimized paths are overlapping under different network sizes and different number of channels. We then present the experimental results which show that both UDP- and TCP-based applications can gain noticeable benefits from our solution.

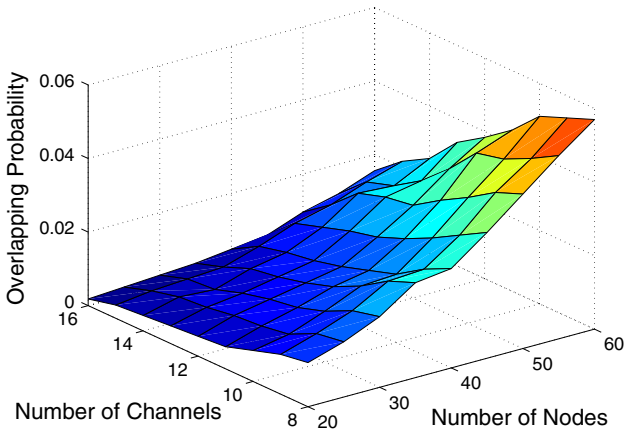

Fig. 7 Probability that the bandwidth- and delay- optimized paths are overlapping in random topology

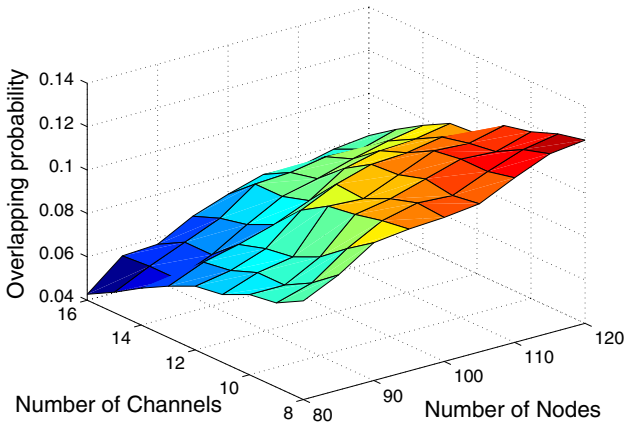

Fig. 8 Probability that the bandwidth- and delay-optimized paths are overlapping in grid topology

6.1 Probability of path overlapping

As discussed earlier, the effectiveness of our solution largely depends on whether the maximum-bandwidth and minimum-delay channel links are overlapped at each hop. Suppose we have N orthogonal channels. For a neighboring node pair, the probability that these two overlap is $1/N$. For a path of L hops, the probability that an overlap occurs is $1 - (1 - 1/N)^L$. For a reasonably large N, say 12, this probability is pretty low. To better understand this, we have also measured this probability in our simulations. We vary the network size from 20 to 60 in the random topologies, and from 80 to 120 in the grid topology. In each topology, the amount of channels is changed from 8 to 16 and we randomly select up to 300 node pairs as sources and destinations.

Figure 7 shows how the probability of path overlapping changes with different number of channels and nodes in random topology. Not surprisingly, it decreases with increasing the number of channels, as more channels potentially offer more disjoint channel links. It increases with increasing the network size, as there are more longer paths in a larger network. Nevertheless, it remains pretty low in all the settings (no more than 6 %).

The results of grid topology are shown in Fig. 8, which follow a similar trend as in the random topologies. An interesting observation is that when the network is larger than a certain size (over 90 in our simulations), the further increase of the overlapping probability becomes marginal. A close investigation shows that at this stage, although the paths in the network may become longer, there are indeed more paths available between node pairs, i.e., paths are more diversified. We thus believe that in practice, the

overlapping probability is still acceptable even with very large network sizes.

6.2 Performance with UDP traffic

We next examine the performance with UDP traffic under different routing protocols. We focus on a typical UDP-based application, that is, video streaming. We use a parameterized version of "Football" video sequence [44] encoded by the H.263 standard. We transmit its I-frames through the minimum-delay path and other frames over the maximum-bandwidth path in JOBD. The rationale is as follows: the I-frames are the most important for video reconstruction because other frames (P- and B-frames) depend on them. To ensure smooth playback, they should be delivered as soon as possible. On the other hand, P- and B-frames are less critical but with relatively larger data volume, and thus should better be transmitted over the maximum bandwidth path. This is particularly true when the GOP (Group of Picture) size is large. In our study, we use a GOP of 8 frames, which is quite conservative. For AOMDV and MWEED, we also use the same scheme to split the traffic among multiple paths. We evaluate the performance in terms of delivery ratio and end-to-end delay under different flow rates.

Figure 9(a) and (b) shows the results with different routing protocols in the random topologies. Note that simulation identifier is the simulation sequence number. For the delivery ratio, JOBD outperforms AOMDV on an average of 39.8 % and MWEED on an average of 11.5 %, while JOBD successfully reduces the end-to-end delay to 65.8 % of AOMDV and 82.2 % of MWEED. This is because JOBD provides both the minimum-delay path and the maximum-bandwidth path, which meet the demands from I-frames and other frames simultaneously. On the other hand, although AOMDV and MWEED also split the traffic among different paths, these paths do not always fit the specific demands from I-frames and other frames, thus resulting in poorer performance.

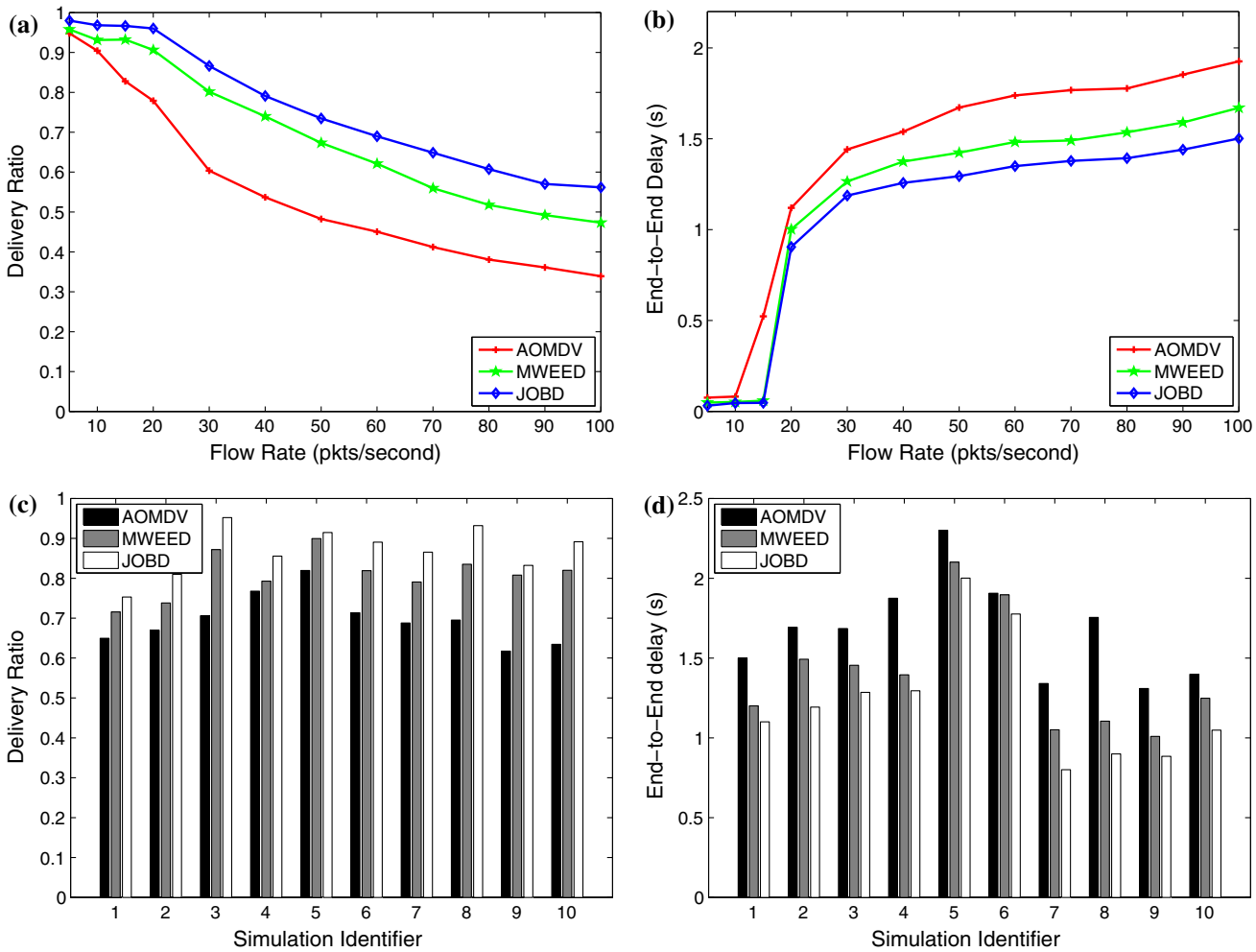

Fig. 9 UDP performance in random topology. (**a**) UDP delivery ratio versus flow rate. (**b**) Average end-to-end delay versus flow rate. (**c**) UDP delivery ratio versus simulation identifier. (**d**) Average end-to-end delay versus simulation identifier

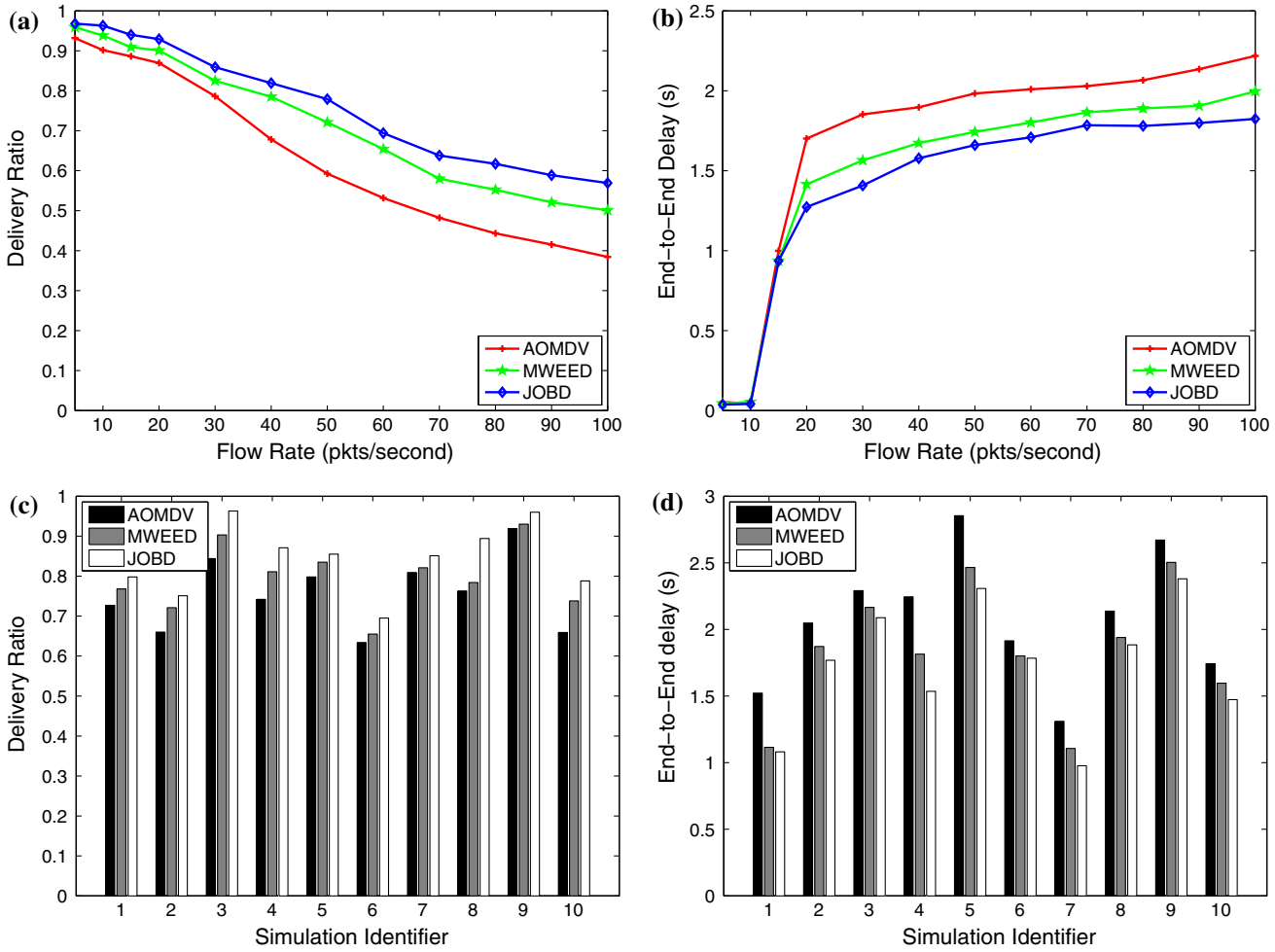

Fig. 10 UDP performance in grid topology. (**a**) UDP delivery ratio versus Flow rate. (**b**) Average end-to-end delay versus flow rate. (**c**) UDP delivery ratio versus simulation identifier. (**d**) Average end-to-end delay versus simulation identifier

Another observation is that although the delivery ratio is decreasing with increasing flow rate, it decreases faster when the flow rate is over 20 pkt/s (Nevertheless, our JOBD remains much better than the other two protocols). The reason is that at this flow rate, the queuing buffers at the intermediate nodes are becoming full and more packets will be dropped if the flow rate increases further. This also explains the sudden change of the end-to-end delay around the flow rate of 20 pkt/s. To better understand this, we further show the performance of different simulation runs at the flow rate of 20 pkt/s in Fig. 9 (c) and (d). It is easy to see that with different random topologies and source destination pairs, the delivery ratio of JODB stays quite stable while the variance of end-to-end delay is more noticeable. This is because the end-to-end delay is more sensitive to the hop distances between the source and destination nodes, which may be quite different for each simulation run.

The results for the grid topology are shown in Fig. 10. It is easy to see that both the delivery ratio and the end-to-end delay follow similar trends as for the random topologies, though the end-to-end delay is generally a bit higher in the grid topology. This is because the grid network has a larger node population, where the hop distances between the source and destination nodes may become longer. Even so, our JODB still performs much better than the other two protocols, with a gain of 10.4–30.3 % on delivery ratio and a gain of 13.7–24.9 % on end-to-end delay.

6.3 Performance with TCP traffic

We next investigate the performance with TCP traffic by an FTP application. we employ TCP-Veno, the most well developed wireless TCP version, which is known for its ability to distinguish wireless loss from congestion. To fully exploit the path diversified multi-QoS optimization in JODB, each file sender transmits as much data as they can with original packets along the bandwidth-optimized path and retransmitted packets along the delay-optimized path, since the retransmitted packets are of relatively small

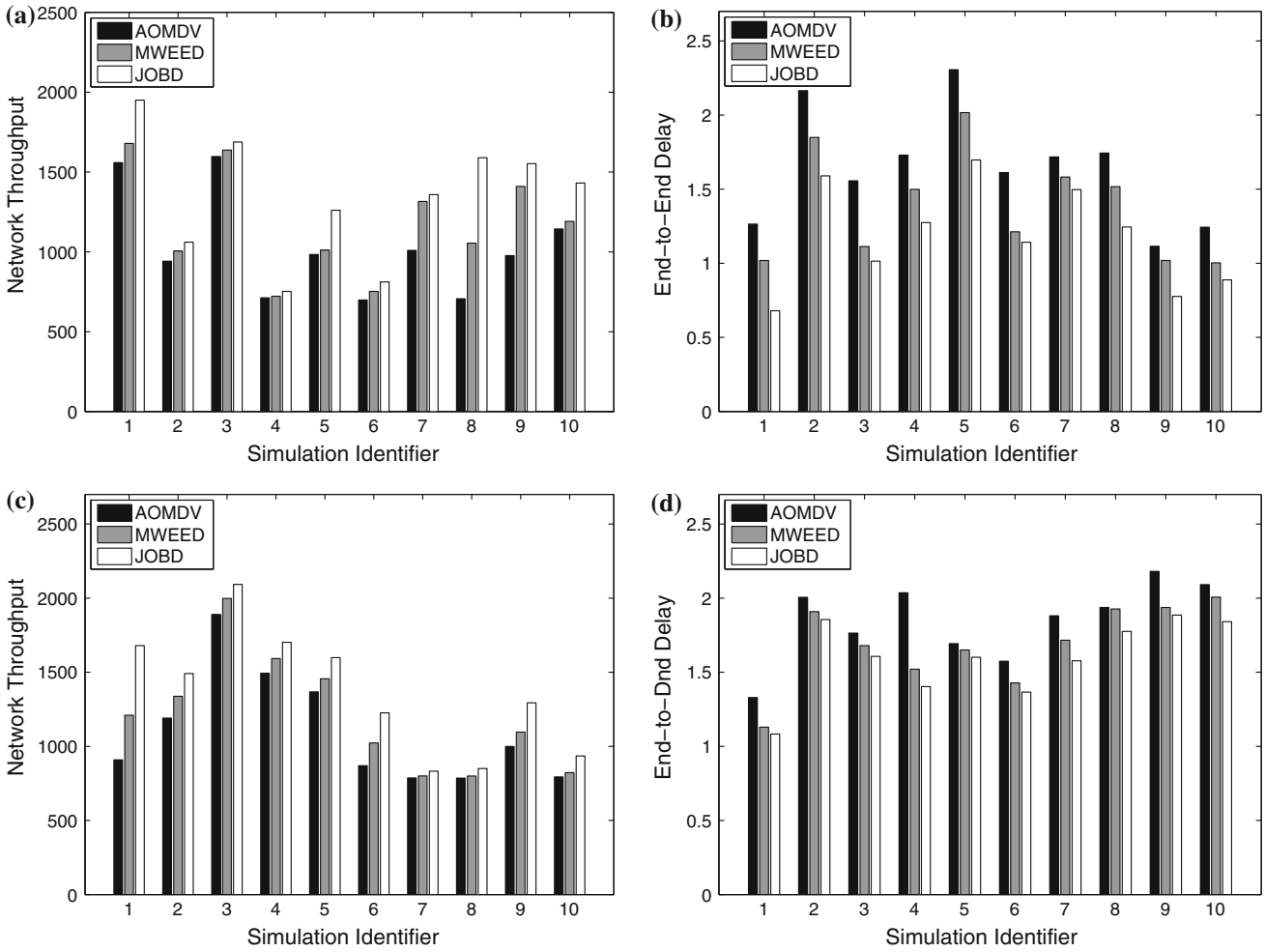

Fig. 11 TCP performance in random and grid topologies. (**a**) Throughput in random topology. (**b**) Average end-to-end delay in random topology. (**c**) Throughput in grid topology. (**d**) Average end-to-end delay in grid topology

amount but have more stringent delay demand while the original packets consume more bandwidth. For AOMDV and MWEED, we also split the traffic and send the original and retransmitted packets along different paths. Figure 11 gives the results in different simulation runs. As expected, in each topology, our JODB achieves the best performance and outperforms the other two on average by 18.8–43.7 and 13.5–27.3 % in terms of throughput and end-to-end delay respectively, since JOBD offers both bandwidth- and delay-optimized paths that can satisfy the requirements for the original and retransmitted packets. Comparing with the results shown in Figs. 9 and 10, one observation is that the throughput of TCP traffic has more noticeable variances among different simulation runs. We believe this is because the reliable transmission and congestion control mechanisms in TCP protocol are more sensitive to the hop distances, which may have great variances for different node pairs and simulation runs.

7 Conclusion and future work

In this paper, we explored the solutions for path diversified multi-QoS optimization in WMNs. We showed that the availability of multiple channels in advanced WMNs sheds new lights into this problem. In particular, we proved that, as long as the best channels with different QoS metrics are not overlapped between neighboring node pairs, complete disjoint paths with different QoS metrics are available. We are particularly interested in the JOBD, the two most common QoS metrics. To this end, we further developed the JOBD protocol. Since the multi-channel environment notably changes the interference pattern from that in single-channel WMNs, our JOBD offered novel estimation tools to achieve much more accurate bandwidth and delay estimation, which take into account the intra-/inter-flow interference as well as channel diversity. We also discussed a series of practical issues toward implementing the JOBD

protocol. To evaluate our solution, we conducted extensive *ns*-2 simulations and compared it with other two state-of-the-art multi-path protocols. The results demonstrated that our JOBD protocol can achieve much better performance with both UDP and TCP traffics.

In the future, we plan to implement our JOBD protocol in real WMNs and conduct more experiments to investigate its interactions with various applications as well as other network services. We are also interested in developing protocols that jointly optimize other QoS metrics besides bandwidth and delay.

Acknowledgments Feng Wang's work is supported by a Start-up Grant from the University of Mississippi.

References

1. Akyildiz, I. F., Wang, X., & Wang, W. (2005). Wireless mesh networks: A survey. *Journal of Computer Networks and ISDN Systems, 47*(4), 445–487.
2. Amir, Y., Danilov, C., Kaplan, M. A., Musaloiu-Elefteri, R., & Rivera, N. (2008). On redundant multipath operating system support for wireless mesh networks. In: *Proceedings of IEEE SECON* (pp. 1–6).
3. Radunovic, B., Gkantsidis, C., Key, P., & Rodriguez, P.(2008). An optimization framework for opportunistic multipath routing in wireless mesh networks. In *Proceedings of IEEE INFOCOM* (pp. 241–245).
4. Tsai, J. W., & Moors, T. (2008). Minimum interference multipath routing using multiple gateways in wireless mesh networks. In *Proceedings of IEEE MASS* (pp. 519–520).
5. Wang, Z., & Crowcroft, J. (1996). Quality-of-service routing for supporting multimedia applications. *IEEE Journal on Selected Areas in Communications, 14*(7), 1228–1234.
6. Wei, W., & Zakhor, A. (2006). Path selection for multi-path streaming in wireless ad hoc networks. In *Proceedings of IEEE ICIP* (pp. 3045–3048).
7. Rong, B., Qian, Y., Lu, K., Hu, R. Q., & Kadoch, M. (2010). Multipath routing over wireless mesh networks for multiple description video transmission. *IEEE Journal on Selected Areas in Communications, 28*(3), 321–331.
8. Manousakis, K., & McAuley, J. A. (2007). Designing OSPF routing areas to meet diverse end-to-end performance. In *Proceedings of IEEE MILCOM* (pp. 1–7).
9. McAuley, A. J., Manousakis, K., & Kant, L. (2008). Flexible QoS route selection with diverse objectives and constraints. In *Proceedings of IEEE IWQoS* (pp. 279–288).
10. Yen, Y. -S., Chao, H. -C., Chang, R. -S., & Vasilakos, A. (2011). Flooding-limited and multi-constrained QoS multicast routing based on the genetic algorithm for MANETs. *Mathematical and Computer Modelling, 53*(11), 2238–2250.
11. Zeng, Y., Xiang, K., Li, D., & Vasilakos, A. V. (2013). Directional routing and scheduling for green vehicular delay tolerant networks. *Wireless Networks, 19*(2), 161–173.
12. Draves, R., Padhye, J., & Zill, B. (2004). Routing in multi-radio, multi-hop wireless mesh networks. In *Proceedings of ACM MobiCom* (pp. 114–128).
13. Yang, Y., Wang, J., & Kravets, R. (2005). Designing routing metrics for mesh networks. In *Proceedings of IEEE WiMesh* (pp. 1–9).
14. Genetzakis, M., & Siris, V. A. (2008). A contention-aware routing metric for multi-rate multi-radio mesh networks. In *Proceedings of IEEE SECON* (pp. 242–250).
15. Li, H., Cheng, Y., Zhou, C., & Zhuang, W. (2009). Minimizing end-to-end delay: A novel routing metric for multi-radio wireless mesh networks. In *Proceedings of IEEE INFOCOM* (pp. 46–54).
16. (2004). *Building the business case for implementation of wireless mesh networks*. San Francisco, CA: Mesh Networking Forum.
17. Vasilakos, A. V., Zhang, Y., & Spyropoulos, T. (2012). *Delay tolerant networks: Protocols and applications*. Boca Raton, FL: CRC Press.
18. Liu, Y., Xiong, N., Zhao, Y., Vasilakos, A. V., Gao, J., & Jia, Y. (2010). Multi-layer clustering routing algorithm for wireless vehicular sensor networks. *IET Communications, 4*(7), 810–816.
19. Spyropoulos, T., Rais, R. N., Turletti, T., Obraczka, K., & Vasilakos, A. (2010). Routing for disruption tolerant networks: Taxonomy and design. *Wireless Networks, 16*(8), 2349–2370.
20. Li, P., Guo, S., Yu, S., & Vasilakos, A. V. (2012). CodePipe: An opportunistic feeding and routing protocol for reliable multicast with pipelined network coding. *Proceedings of IEEE INFOCOM* (pp. 100–108).
21. Youssef, M., Ibrahim, M., Abdelatif, M., Chen, L., & Vasilakos, A. V. (2013). Routing metrics of cognitive radio networks: A survey. *IEEE Communications Surveys and Tutorials, PP*(99), 1–18.
22. Wang, Z., & Crowcroft, J. (1991). Finding disjoint paths in networks. *ACM SIGCOMM Computer Communication Review, 21*(4), 43–51.
23. Chen, J. C., Chan, S. H., & Li, V. (2004). Multipath routing for video delivery over bandwidth-limited networks. *IEEE Journal on Selected Areas in Communications, 22*(10), 1920–1932.
24. Misra, S., Xue, G., & Yang, D. (2009). Polynomial time approximations for multi-path routing with bandwidth and delay constraints. In *Proceedings of IEEE INFOCOM* (pp. 558–566).
25. Zhang, W., Tang, J., Wang, C., & Soysa, S. (2010). Reliable adaptive multipath provisioning with bandwidth and differential delay constraints. In *Proceedings of IEEE INFOCOM* (pp. 1–9).
26. Tarn, W., & Tseng, Y. (2007). Joint multi-channel link layer and multi-path routing design for wireless mesh networks. In *Proceedings of IEEE INFOCOM* (pp. 2081–2089).
27. Zeng, K., Yang, Z., & Lou, W. (2010). Opportunistic routing in multi-radio multi-channel multi-hop wireless networks. *IEEE Transactions on Wireless Communications, 9*(11), 3512–3521.
28. Jain, M., Choi, J., Kim, T., Bharadia, D., Seth, S., Srinivasan, K., et al. (2011). Practical, real-time, full duplex wireless. In *Proceedings of ACM MobiCom* (pp. 301–312).
29. Choi, J., Jain, M., Srinivasan, K., Levis P., & Katti, S. (2010). Achieving single channel, full duplex wireless communication. In *Proceedings of ACM MobiCom* (pp. 1–12).
30. Fang, X., Yang, D., & Xue, G. (2011). Distributed algorithms for multipath routing in full-duplex wireless networks. In *Proceedings of IEEE MASS* (pp. 102–111).
31. Wu, D., & Mohapatra, P. (2010). From theory to practice: Evaluating static channel assignments on a wireless mesh network. In *Proceedings of IEEE INFOCOM* (pp. 1–5.)
32. Avallone, S., Akyildiz, I. F., & Ventre, G. (2009). A channel and rate assignment algorithm and a layer-2.5 forwarding paradigm for multi-radio wireless mesh networks. *IEEE/ACM Transactions on Networking, 17*(1), 267–280.
33. Subramanian, A. P., Gupta, H., Das, S. R., & Cao, J. (2008). Minimum interference channel assignment in multiradio wireless mesh networks. *IEEE Transactions on Mobile Computing, 7*(12), 1459–1473.
34. Kyasanur, P., & Vaidya, N. H. (2006). Routing and link-layer protocols for multi-channel multi-interface ad hoc wireless networks. *SIGMOBILE Mobile Computing and Communications Review, 10*(1), 31–43.
35. Phatak, D. S., & Goff, T. (2002). A novel mechanism for data streaming across multiple IP links for improving throughput and reliability in mobile environments. In *Proceedings of IEEE INFOCOM* (pp. 773–781).

36. Luo, W., Balachandran, K., Nanda, K., & Chang, K. K. (2005). Delay analysis of selective-repeat ARQ with applications to link adaptation in wireless packet data systems. *IEEE Transaction on Wireless Communications, 4*(3), 1017–1029.
37. Sarr, C., Chaudet, C., Chelius, G., & Lassous, I. G. (2008). Bandwidth estimation for IEEE 802.11-based ad hoc networks. *IEEE Transactions on Mobile Computing, 7*(10), 1228–1241.
38. Cheng, H., Xiong, N., Vasilakos, A. V., Yang, L. T., Chen, G., & Zhuang, X. (2012). Nodes organization for channel assignment with topology preservation in multi-radio wireless mesh networks. *Ad Hoc Networks, 10*(5), 760–773.
39. (1999). Wireless lan medium access control (MAC) and physical layer (PHY) specifications. *ANSI/IEEE Std* 802.11: 1999 (E) Part 11, ISO/IEC 8802-11.
40. Cheng, Y., Ling, X., Song, W., Cai, L., Zhuang, W., Shen, X. (2007). A cross-layer approach for WLAN voice capacity planning. *IEEE Journal on Selected Areas in Communications, 25*(4), 678–688.
41. Marina, M. K., & Das, S. R. (2001). On-demand multipath distance vector routing in ad hoc networks. In *Proceedings of IEEE ICNP* (pp. 14–23)..
42. Couto, D., Aguayo, D., Bicket, J., & Morris, R. (2003). A high-throughput path metric for multi-hop wireless routing. In *Proceedings of ACM MobiCom* (134–146).
43. Wu, Z., Ganu, S., & Raychaudhuri, D. (2006). IRMA: Integrated routing and MAC scheduling in multi-hop wireless mesh networks. In *Proceedings of IEEE WiMesh* (p. 10).
44. Puri, R., Lee, K., Ramchandran, K., & Bharghavan, V. (2001). An integrated source transcoding and congestion control paradigm for video streaming in the internet. *IEEE Transactions on Multimedia, 3*(1), 18–32.

X. Guo received the B.Sc. degree in Telecommunication Engineering from Jilin University, Changchun, China, in 2007, and the M.Sc. degree in computer science from Simon Fraser University, Burnaby, British Columbia, Canada, in 2011. Her research interest is wireless mesh network.

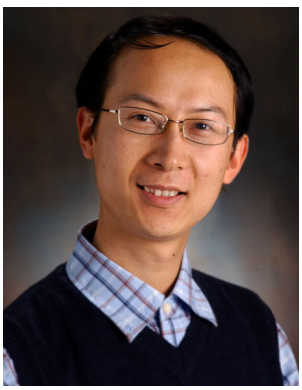

F. Wang received both the Bachelor's degree and Master's degree in Computer Science and Technology from Tsinghua University, Beijing, China in 2002 and 2005, respectively. He received the Ph.D. degree in Computing Science from Simon Fraser University, Burnaby, British Columbia, Canada in 2012. He is a recipient of the Chinese Government Scholarship for Outstanding Self-financed Students Studying Abroad (2009) and IEEE ICME Quality Reviewer Award (2011). He is currently an Assistant Professor in the Department of Computer and Information Science at the University of Mississippi, University, MS, USA. His research interests include wireless mesh/sensor networks, cyber-physical systems, peer-to-peer networks, socialized content sharing and cloud computing. He is a member of IEEE. He serves as TPC member in various international conferences such as IEEE/ACM IWQoS, ACM Multimedia, IEEE ICC, IEEE GLOBECOM, IEEE CloudCom and IEEE ICME.

J. Liu received the B.E. degree (cum laude) from Tsinghua University, Beijing, China, in 1999, and the Ph.D. degree from The Hong Kong University of Science and Technology in 2003, both in computer science. He is a co-recipient of ACM TOMCCAP Nicolas D. Georganas Best Paper Award 2013, ACM Multimedia Best Paper Award 2012, IEEE Globecom 2011 Best Paper Award, and IEEE Communications Society Best Paper Award on Multimedia Communications 2009. He is currently an Associate Professor in the School of Computing Science, Simon Fraser University, British Columbia, Canada, and an EMC-Endowed Visiting Chair Professor of Tsinghua University, Beijing, China. He was an Assistant Professor in the Department of Computer Science and Engineering at The Chinese University of Hong Kong from 2003 to 2004. His research interests include multimedia systems and networks, cloud computing, social networking, wireless ad hoc and sensor networks, and peer-to-peer and overlay networks. He serves on the editorial boards of IEEE Transactions on Multimedia, IEEE Communications Surveys and Tutorials, and IEEE Internet of Things Journal. He is a TPC co-chair of IEEE/ACM IWQoS'14 and an Area Chair of ACM Multimedia'14.

Y. Cui received the B.E. degree and the Ph.D. degree from Tsinghua University, China in 1999 and 2004, respectively. He is currently a full professor in Tsinghua University, Council Member in China Communication Standards Association, Co-Chair of IETF IPv6 Transition WG Softwire. Having published more than 100 papers in refereed journals and conferences, he received the National Science and Technology Progress Award of China in 2005, the Influential Invention Award of China Information Industry in both 2012 and 2004, best paper awards in ACM ICUIMC 2011 and WASA 2010. He authors 3 Internet Standard Documents including RFC 5565 and RFC 7040 for his proposal on IPv6 transition technologies. He serves at the Editorial Board on both IEEE TPDS and IEEE TCC. His major research interests include mobile wireless Internet and computer network architecture.